Research Article GU J Sci 38(2): x-x (2025) DOI: 10.35378/gujs.1469645

Gazi University

Journal of Science

http://dergipark.gov.tr/gujs

Vertical Stirred Mill (VSM) Welding Machine Design

Aydin SIK[1,*], Ali AKAR[2]

[1]Gazi University, Faculty of Architecture, Ankara, Türkiye
[2]Birikim Engineering and Industrial Contracting Inc., Birikim Engineering Design Center, Ankara, Türkiye

Highlights

- This paper focuses on vertical stirred mill technology.
- Vertical stirred mill welding processes were investigated.
- The weld seam qualities were investigated by examining the weld seams made with the designed machine.

Article Info

Received: 17 Apr 2024
Accepted: 15 Jan 2025

Keywords

Vertical stirred mills
Submerged arc welding
Welding

Abstract

Vertical stirred mills are widely used in the mining industry because they are more efficient than traditional drum mills. Vertical agitation grinders are used in secondary, regrinding, and fine grinding applications in the mining industry because of their energy efficiency, cost savings and small footprint. The solid welding of the mixer leaves to the body plays an important role in terms of wear, maintenance planning, and operating costs. The grinder must be resistant to the strains during mixing and maintain its rigidity. In vertical mixer grinders, it is difficult to weld the screw leaves to the shaft in a helical manner. In this study, a Screw Welding Machine (WSM) was designed to weld the vertical stirred grinder leaves to the body to meet this difficulty. In order to perform welds between adjacent leaves and corners, using a submerged arc welding machine, a welding bench has been designed. Designed bench enable to connect seven different sizes of vertical mixer grinders to WSM. Designed WSM compansate deformations caused bey weld induced heat by changing part position and opposite side weld application. The designed bench remains stationary during welding procedure. The weld seam qualities were investigated by examining the weld seams made with the designed machine (spectral analysis, hardness measurement, notch impact resistance, macro examination, and metallography examination).

1. INTRODUCTION

Vertical stirred mill technology has been preferred over ball heaters for the last 20 years because of its superior energy efficiency [1-3]. Vertical stirred mills are recently widely used in many sectors such as the mining industry [4]. Results of research studies about this process proven that this technology to be highly energy efficient, for both of fine and coarse mixers with with greater opportunities for future optimization [5-8]. As a result, a need arises for reduced particle size processing that can facilitate the relase of valuable minerals for post-concentration stages. In this context, additional power is required to achieve a finer grain size. Therefore, grinding and regrinding applications are increasing in importance [9-12].

Nowadays the fact that vertical stirred mills are widely used in the mineral industry, the increasing variety of models from different manufacturers, and the number of new units installed worldwide are evidence of the increasing interest in these mills. With so many options available during the design phase of a faciliy, choosing the most suitable mill for a particular application becoming more difficult than ever [13-14].

For secondary regrind, and fine grinding applications vertical stirred milling is a well-recognized technology and is increasingly replacing coarser ball mill applications in the secondary and tertiary fields. The driving force for this development is that higher energy efficiency can be achieved with vertical stirred mill [15-17].

*Corresponding author, e-mail:aydins@gazi.edu.tr

When designing a vertical stirred mill, the work required from the mixer (mixing speed, capacity), properties of the material to be mixed, work safety, economy, and efficiency can be considered as a whole. Design should be carried out by determining the priority issues and taking care of all their effects. The amount of ground is significant in the design of a quatity yield. More detailed studies on the material's grain size, grain geometry, material fluidity, material hardness, material compressibility, chemical properties, and explosiveness of the material, and the development of experimental and empirical methods play an important role in the design of screw mixers.

One of the parameters used in the manufacturing of mixer screws is the submerged arc welding method used to weld the leaves to the shaft, shown in Figures 1 and 2 welding parameters are welding current, arc voltage, wire advancement speed, welding speed and electrode protrusion. By choosing this parameters correctly and with sensitivity, well appearance of weld seams can be achieved, in the submerged arc welding method [18-22].

One of the methods developed for welding processes of materials with high wall thickness is the Submerged Arc Welding method. In this method, the arc column and the weld seam are protected against external factors by the effect of the powder charged from just in front of the welding torch or around the electrode inside the torch during the welding process, and high heat input can be obtained by preventing heat loss. In addition to high current application and energy efficiency, the formation of phases that cause embrittlement can be prevented even at high current values due to the slow cooling provided as a result of both the powder and the slag covering the weld seam.

Since the electrode of the same diameter used in this method is loaded with a higher welding current compared to welding with normal covered electrode, a larger weld pool and deeper penetration are achieved. Since the method is also suitable for semi-automatic and fully automatic welding applications, it has found widespread use in industrialized countries as a modern welding application [23-28].

Figure 1. *Submerged arc welding method*

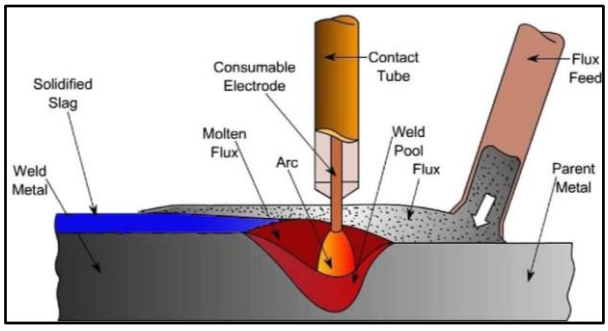

Figure 2. *Submerged arc welding chart*

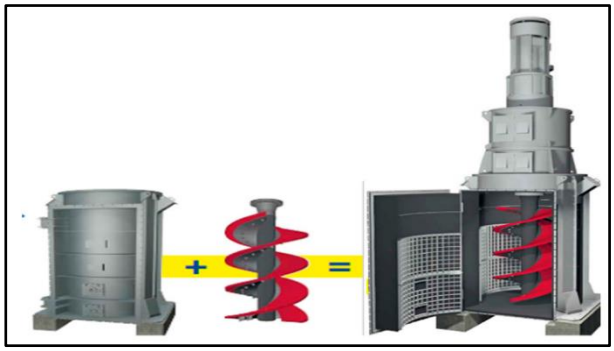

Figure 3. *Schematic of Tower and Vertical mill [29]*

The tower and vertical mill consist of a vertically positioned body and rotating helical blades. In this type of mixing mill, the movement of the material begins with the rotation of the helical wheel in the system. Shown in Figures 3 tower and vertical mills are often used in closed circuit with small hydrocyclones for regrinding in mineral processing applications. These mills provide limited grinding size (d_{80} 20µm) as they use standard 12 mm media. Although the energy efficiency applied to the grains increases when using smaller media, the use of media smaller than 12 mm causes a problem such as balls escaping from the top of the mill during grinding [29, 30].

2. MATERIAL METHOD

2.1. Materials and Experimental Methods

In this study, test samples were made at Birikim Engineering Design Center in Ankara. Welding operations were carried out on the Vertical Stirred Mill (VSM) Welding Bench, specially designed by the company, and then test samples were prepared. In this designed machine, the same and double-sided welding of screws was carried out automatically.

When the welding parameters are selected appropriately, error-free, and well appearance of weld seams can be obtained. Because the arc takes place under the welding dust during the welding process, there is no need to use a mask to protect from arc rays. No harmful metal dust or smoke is formed during welding. Since its deep processing ability is good, it allows welding up to 16 mm thickness without opening narrow and deep welding bevels and up to 30 mm thickness in double-sided welding. Although it is suitable for semi-automatic and fully automatic applications, it can also be applied manually if desired [31-34].

In this study, the design of a submerged arc welding bench for welding mixer screw leaves to the shaft is shown in Figure 4.

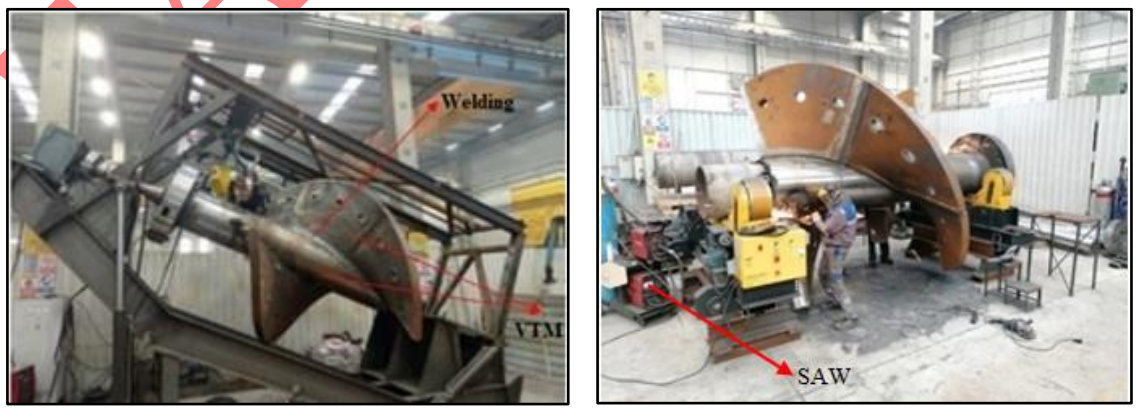

Figure 4. *Welding process of spirals*

The cast leaves and wings produced for mixing screws have a uniform thickness. The screw is formed by welding a sufficient number of profile blades onto the central shaft of the cast screw leaf [35-39]. The first

weld seam was made with a gas arc welding machine (MIG/MAG). Then, the welding parameters of the submerged arc welding machine (welding current, arc voltage, wire advancement speed, and welding speed) were determined, and the welding process was carried out. In this study, the parameters of a submerged arc welding for welding mixer screw leaves to the shaft is shown in Table 1-5.

Table 1. *Chemical composition of spindle and leaf material of S355 JR*

Element content (%)										
C	S	Al	Si	P	V	Cr	Mn	Ni	Cu	Mo
0.188	0.003	0.0273	0.2314	0.0051	0.00327	0.1571	1.053	0.0548	0.0575	0.0297

Table 2. *Chemical composition of welding fluxes used in submerged arc welding machine*

Material	Chemical Composition (%)								
	SiO_2	MnO	MgO	CaF_2	Na_2O	Al_2O_3	CaO	TiO_2	Metal alloy
FX860-25	19	11	17	12	2	32	2	2	3 max.

Table 3. *Chemical analysis of the electrode used in the gas welding machine*

Elektrot	Chemical Composition (%)										
	C	Mn	Si	P	S	Cr	Ni	Mo	Cu	Ti	Al
AS SG3	0,080	1,690	0,970	0,013	0,012	0,040	0,050	0,010	0,190	0,001	0,007

Table 4. *Chemical analysis of the electrode used in the submerged arc welding machine*

Elektrot	Chemical Composition								
	C	Mn	Si	P	S	Cr	Ni	Mo	Cu
AS S2	0,095	0,900	0,080	0,011	0,012	0,037	0,025	0,017	0,190

Table 5. *MAG and Submerged arc welding machine welding parameters*

Paso number	Method	Current (A)	Voltage (V)	Welding Speed (mm/min)	Wire diameter (mm)	Current type	Welding powder	Gas Heat input (KJ/mm)
1-2 (MIG/MAG)	135	258-260	28-29	10,21/124-135	1,2	DC(+)	M24	2,57-2,52
3-37 (SMAW)	121	520-570	27,5-27,6	200-380	4,0	DC(+)	FX860-25	2,26-2,48
38-68 (SMAW)	121	520-578	27,6	200-240	4,0	DC(+)	FX860-25	3,59-4,79

2.2. Welding Processes

Vertical stirred mills are produced by spirally welding a cast steel sheet to the body of a shaft. Cast steel sheets are prepared in desired dimensions for welding. The pitch is then marked on the shaft, and the reference helix is drawn. The welding process of the leaves placed in this reference spiral begins on the bench. In mixer screws, while the leaf is welded to the shaft, many welding seams are made on top of each other. Since the first and second weld seams are made with MIG/MAG welding, most of the weld spatter and slag are removed, but the weld is not ground (Figures 6 and 7). After the second welding seam, the welding seams are made by the Submerged Arc Welding (SAW) method. A total of sixty-six welding seams are applied, thirty-three from one side. After the welds are visually inspected, the parts with protrusions and burrs deemed necessary are coarsely ground. This seam improves the appearance of the welds and usually comes at no additional cost.

Figure 5. *Welding process*

Figure 6*. Weld seams*

2.3. Designed Welding Automation System

With the welding automation application, SAW (automation system in the submerged arc welding machine) and all welding devices used in the production stages can be controlled on a single screen. Additionally, the parameters used are reported and recorded. Thus, welding processes are no longer dependent on the operator, and continuity in the production of VSM mixing screws of the same quality is ensured. In addition, the operator cost, one of the highest costs in welding operations, has also been reduced. Figure 7 shows motion sensor signals managed by PLC (programmable logic controller), rotation signals, and welding parameters such as current, voltage, and wire speed on the welding automation control unit screen.

Figure 7. *Designed submerged arc welding machine apparatus*

Touch screens were used in the system to facilitate operator use. Data collected from welding machines can be displayed on operator screens. Thanks to the user management system, access and control to the parameters of the welding machines are limited, ensuring that operators can only access the parameters permitted by the administrator or service engineer. All parameters of the welding machine can be changed on the operator screen and stored in tables in the PLC memory according to the specific product type and number for later reuse. Welding quality is achieved by always maintaining a constant wire-weld metal distance despite the high accuracy and repeatability capacity of the welding system and the oval weld metal

shape. In the welding automation system, a closed camera and screen system allows the operator to monitor the weld, especially in small-scale product production visually. Thus, it offers remote access and control of the system. These cameras, used separately for internal and external welding, can be monitored on the operator panel, and continuity in weld point tracking can be ensured by horizontal and vertical alignment.

2.4. Visual Inspection of Welded Plates (Sheets)

A visual inspection was carried out to detect superficial defects that may be seen after the welding process in the welded connections where the test samples will be prepared. This inspection was based on "ANSI/AWS D9.1-90 Sheet Metal Welding Code". The seam height formed, the seams formed on the seams, combustion grooves, spatters, seam root sagging, as well as the seam width and insufficient melting areas that may occur at the root after welding were visually examined in detail, and it was observed that the spatters and other issues were within the acceptable limits. It is given visually in Figure 6.

2.5. Test Sample Removal Principles

After the welding process, the samples were allowed to cool under normal cooling conditions as per the relevant standards. Test samples in accordance with EN-288-3 were prepared according to the test plan made from these plates that passed visual inspection. 25 mm sections from the beginning and end of the welded plates were cut and discarded. In this way, errors that may occur at the beginning and end of the weld are prevented.

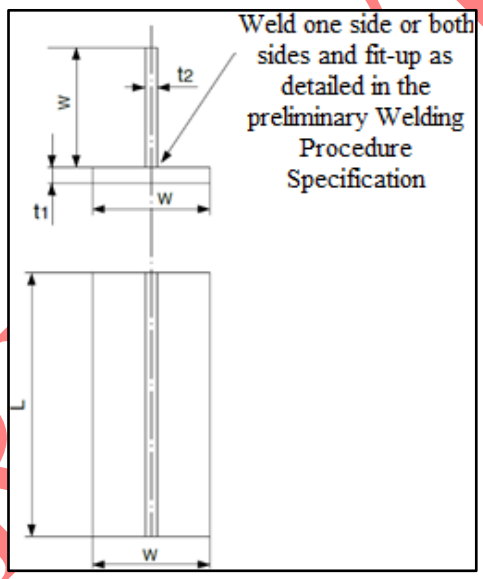

Figure 8. *Dimensions and types of test assembly for fillet welds*

Distribution plan of samples on the plate according to EN 288-3. All the dimensions are in mm, unless otherwise indicated (Figure 8).

3. FINDINGS and DISCUSSION

3.1. Spectral Analysis Experiment

The spectral analysis experiment was carried out in an environment with a temperature of 20±2 ^{0}C and relative humidity of 50±30% in accordance with the ASTM E415 standard. Spectral analysis is an analysis method used to determine the chemical components or elements of a material through light. Optical Emission Spectrometry (OES) is a device that performs this type of analysis. The main purpose of OES is to determine the elements contained in the material and their concentrations. This information is used to control the quality of the material, analyze its composition, monitor metallurgical processes, and characterize materials used in industrial production. OES is frequently used in industrial applications, especially metallurgy, metal foundries, steelmaking, aluminum and iron ore analysis, hot metal analysis,

and mass spectrometry. It is also widely used in chemical analysis, materials science, and metallurgical research in research laboratories and universities.

Table 6. *Samples*

Sample No	Material type	Quality
P.1511W	Weld	5355J2
P.1511M	Material	S355J2

Table 7. *Spectral analysis results*

No	Δ	%C	%Si*	%Mn*	%P*	%S*	%Cr*	%Mo*	%Ni*	%Ar	%Cu*	%Nb	%V*	%W	%Pb	%Bi	%Sb	%B	%N	%Fe
P.1511 W	2	0.0612	0.1695	1.0308	0.0289	0.0142	0.0337	0.3825	0.0317	0.0107	0,0874	0.0005	0.0079	0.0032	0.0003	0.0002	< 0.0004	0.0001	0.0048	98.1319
P.1511 M	2	0.1440	0.0295	0.4371	0.0154	0.0146	0.0453	0.0046	0.0231	0.0364	0.0445	< 0.0002	0.0044	0.0015	< 0.0002	< 0.0002	< 0.0004	< 0.0001	< 0.0004	99.1981

Δ: number of measurements
*These elements are within the scope of TÜRKAK accreditation.

If the values of one or two of the alloying elements such as Mn and Si in S355 JR steel do not exceed at least 1,65% Mn and 0,60% Si and if the chemical composition does not require the presence of any other alloying element in a certain amount, these steels are classified as carbon steels. It is used in the construction and industrial sectors for making box profiles, bars and hot rolled industrial profiles (Table 6, 7).

3.2. Hardness Profile Test Report (Vickers Hardness Test according to TS EN ISO 9015)

Micro Hardness Screening

Hardness screening is carried out on the samples taken from all welded joints with a Vicker hardness measuring device (Instron Wolpert) along a line, as seen in Figure 9. While measuring hardness, the base metal, heat-affected zone (HAZ), and weld metal values were taken by scanning double-sided, at as symmetrical intervals as possible, according to the weld center line.

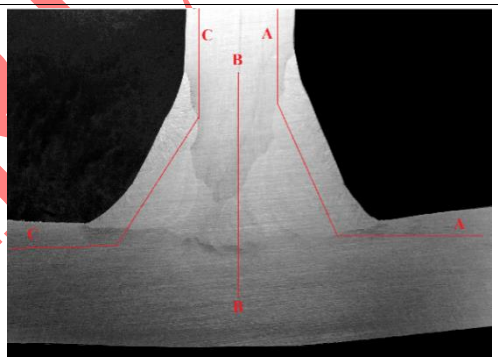

Hardness:1	Main Material			HAZ			Weld Metal			HAZ			Main Material		
Point	**1**	**2**	**3**	**1**	**2**	**3**	**1**	**2**	**3**	**1**	**2**	**3**	**1**	**2**	**3**
Series A-A	154	147	147	171	169	210	196	196	204	166	142	145	142	143	145
Series B-B	141	146	146	144	146	158	181	185	190	208	169	160	148	146	146
Series C-C	133	141	140	136	139	168	187	191	204	198	147	145	138	135	135

Figure 9. *Hardness values (HV 10)*

Figure 9 shows the microhardness values of S355JR connection combinations joined by SAW welding method. The highest hardness values were measured in the weld metal and Heat Affected Zone (HAZ) in Series A-A, in the weld metal and HAZ in Series B-B, and in the weld metal and HAZ in Series C-C.

When the measured hardness values are examined, it is seen that there is not much difference between weld metals and HAZs. In Series A-A, it was determined that the hardness value was highest in the HAZ. It can be said that the higher hardness values of weld metal and HAZs than the main material are due to different cooling rates after welding depending on the heat input during welding. Benedetti [34] joined S355JR structural steel by welding and reported similar results in hardness tests.

The high hardness values detected in the weld seam region are seen to be due to the chemical structure of the electrode. The high carbon content in the filler metal explains why the hardness value increases. Since the carbon ratio in the composition of normal steel is generally (less than 0.2%), martensite does not form in the heat affected zone (HAZ) during welding. Due to the lack of martensite formation, the metal in the heat affected zone (HAZ) region increases to high temperature values and causes the formation of large grains. The metal that cools after the high temperature will form an area with lower hardness and higher strength.

3.3. Notch Impact Test Report according to TS EN ISO 9016

Table 8. *Notch impact test results according to TS EN ISO 9016 (10x10x55mm)*

No	Name	Location of the notch	KV-Pulse absorption energy (J)	Observed defects, type and dimensions
IT1	VWT	welding	57,29	There is no discontinuity
IT2	VWT	welding	57,74	There is no discontinuity
IT3	VWT	welding	51,40	There is no discontinuity

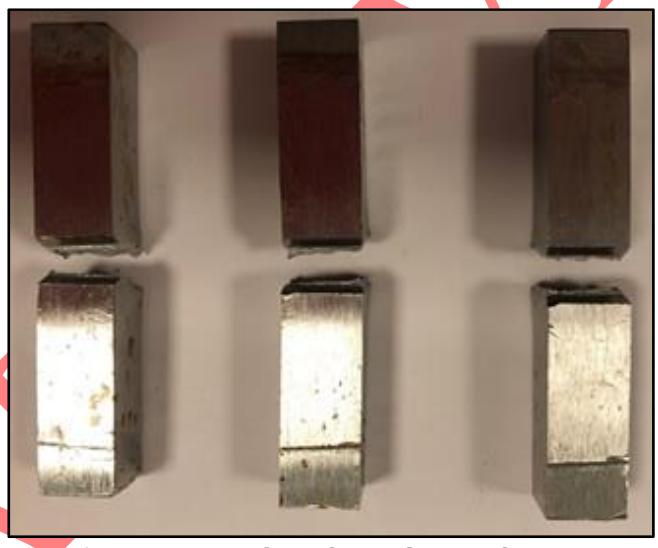

Figure 10. *Samples subjected to notch testing*

In the study, notch impact samples arranged in appropriate sizes were tested in pieces at -20 ^{0}C. The average notch impact toughness of the welded drive was determined to be 55 J. According to the data in Table 8 and Figure 10, it has been determined that the welded joints are safe against dynamic stresses since the broken fracture energy values are higher than the 27 J (-20 ^{0}C) value stipulated by the standard for energy sources and weld metal [40-44].

3.4. Metallographic Examination

In order to get the most realistic results from all welded connections, the samples are generally selected to represent the structure. After a visual inspection of the weld seams, a hand saw was used to prevent the cutting-generated heat. After the surfaces of the cut samples were cleaned, cold embedding was performed according to the sample sizes, and polyester was used in cold embedding. Then, the samples were polished, and Alumina was used as an abrasive for fine polishing.

After fine polishing with alumina, the etching process was started. During the etching process, all kinds of acids and other residues were removed from the samples, immersed in 5% Nital and kept for 30-60 seconds by washing them with alcohol. Then, it was dried thoroughly with a hot air blower (hair dryer). Internal structure images of the test samples (Metal microscope and SEM) were taken. The macrostructure can be seen in Figure 11.

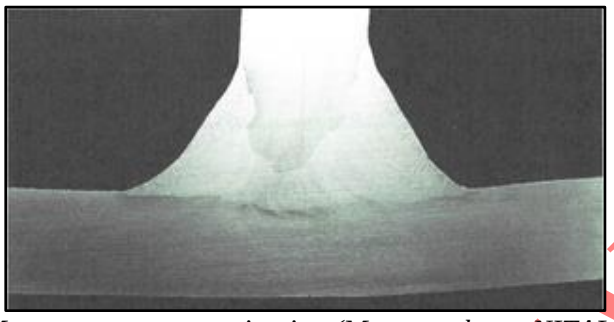

Figure 11. *Macro structure examination (Macro etchant: NITAL 5%)*

The results of the macrostructure examination of the weld seam cross-section obtained from the macro examination samples taken from the region of the welded plates specified in Figure 11 are given in Figure 3. Accordingly, it has been determined that there are no defects such as pores, slag residue, melting deficiency, interpass melting deficiency or merging defect, burning groove, etc., and defects such as linear misalignment, excessive weld metal according to TS EN ISO 5817 standard are at acceptable levels even in B class. Only laminar cracking caused by the production of the base material is observed.

3.5. Microstructure Examination

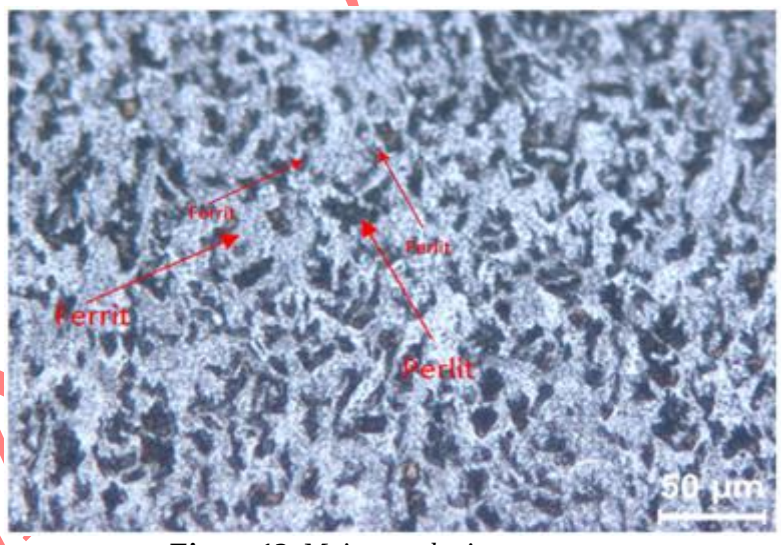

Figure 12. *Main metal microstructure*

Figure 12 shows that there are ferrite and pearlite phases in the structure of the main material. The black regions in the microstructure represent pearlite, and the light regions represent ferrite. Due to the low carbon content in the microstructure, the pearlite content is low. Accordingly, the ferrite content is high.

Figure 13. *Upper region HAZ (Heat Affected Zone) A-A section*

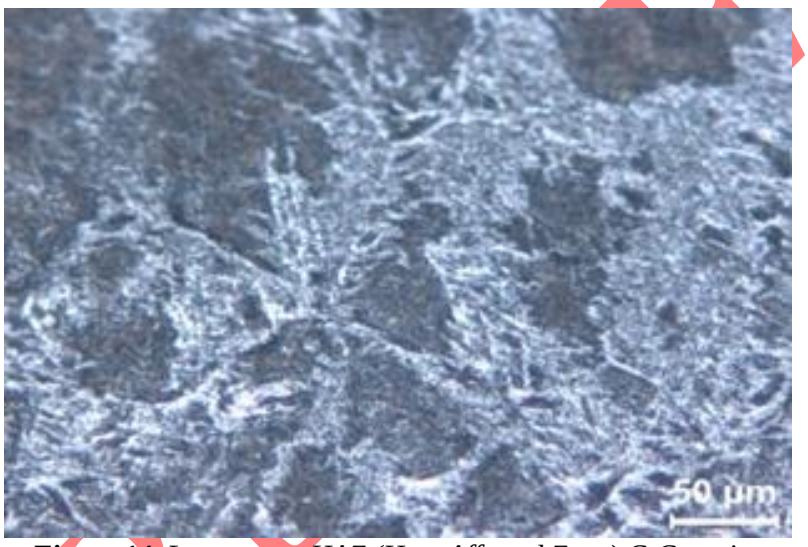

Figure 14. *Lower zone HAZ (Heat Affected Zone) C-C section*

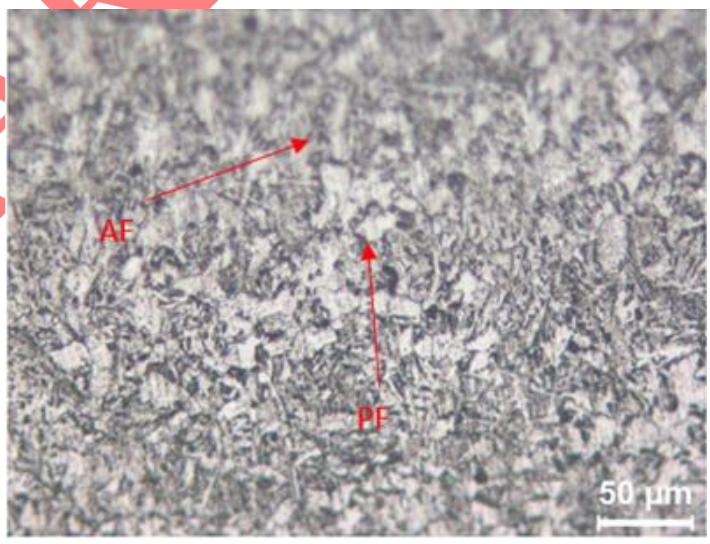

Figure 15. *Weld metal*

As seen in Figures 13-15, the microstructure of the base metal is different from the microstructure of the weld metal. The difference in the microstructure is not related to the chemical composition but to the

different thermal histories of the base metal and the weld metals. It was determined that there were needle-like and polygonal ferrite structures in the weld metal microstructures.

Acicular ferrite is formed by nucleation in the inner part of austenite grains. This structure formed by nucleation increases the strength of the weld seam. In addition, the structure formed by this nucleation increases the toughness of the weld seam. According to the research, acicular ferrite is formed as a fine-grained structure. Due to the formation of the fine-grained structure, there is a decrease in cracks formed by splitting.

The microstructure of the structural steel S355JR joined by submerged arc welding method is shown in Figure 15. As seen in the microstructure, the light-colored parts show ferrite and the dark areas show pearlite. In this microstructure, sufficient information can be obtained about the number of components in the steel. This shows that the ferrite phase in the low carbon is high. On the other hand, the pearlite phase is seen to be low. Akkaş et al. determined that there is ferrite in the white colored parts according to the 0.09% carbon content in the microstructure of S235JR. They stated that pearlite is seen very little in the darker areas in the microstructure [45-48].

Acicular ferrite is also characterized by high-angle boundaries between ferrite grains. This further reduces the possibility of splitting because these boundaries prevent crack propagation. The nucleation of various ferrite morphologies is reported to be aided by non-metallic inclusions. In particular, it has been described that oxygen-rich inclusions of a certain type and size are associated with the intragranular formation of acicular ferrite [49-52]. Polygonal ferrite is formed when austenite grains come together. It is seen that it damages toughness because it is formed from austenite grains. Literature shows that polygonal ferrite is formed as coarse ferrite islands within the previous austenite grains. Polygonal ferrite has been found to damage toughness because it is formed from coarse grain size [53-59].

3.6. SEM Review

The appearance of the fractured surfaces resulting from the notch test, the structure of S355 JR steel, and its continued exposure to ductile fracture due to its low carbon properties are separated in Figure 16.

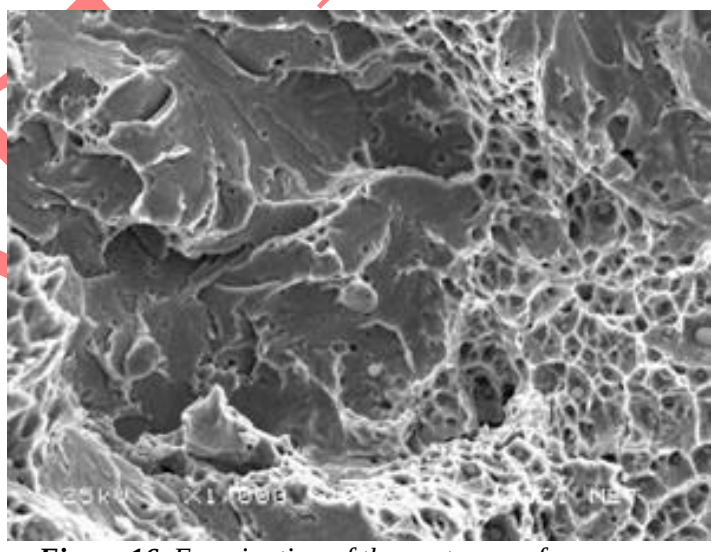

Figure 16*. Examination of the rupture surface*

As described in literature studies, mechanical instability of the sample or void incorporation can lead to fracture. First, voids nucleate in inclusions and then grow with the help of plasticity. When they finally meet, a crack forms, and the material breaks. It is stated that ductile fracture occurs in the S355 J2 sample subjected to plastic deformation [56-67].

4. RESULTS AND RECOMMENDATIONS

In this study, the solution to the problems encountered while welding the leaves to the shaft in vertical stirred mills screws was examined in detail, and a submerged arc welding bench was designed for this purpose. With this design,

-Two-sided welding of the screw leaf to the shaft can be done sequentially. Thermal deformations caused by one-sided welding have been controlled and eliminated.
-Welding operations, previously done by four operators, can now be done by one operator in a shorter time.
-A decrease in the cost of the welding process has been achieved by reducing the number of operators.
-All welding processes can be viewed and controlled on a single screen.
-Welding parameters are reported, recorded, and typified. Thus, uniformity and continuity in welded production quality are ensured.
-Operator-related welding errors have been reduced.
-Continuity has been ensured in the production of the same high-quality VSM mixing screw.

The difference seen in the microstructure is not related to the chemical composition but to the different thermal histories of the base metal and weld metals, and acicular and polygonal ferrite structures had been detected in the weld metal microstructures of the samples. Acicular ferrite is formed by direct nucleation on inclusions in the inner part of austenite grains and increases the strength and toughness of the weld metal.

The image of the base material microstructure of S355J2 shows that there are ferrite and pearlite phases in the base material structure. The black regions in the microstructure represent pearlite, and the light regions represent ferrite. Due to the low carbon content in the microstructure, the pearlite content is low. Accordingly, the ferrite content is high.

The average notch impact toughness of the welded connection was determined to be 55 J. It has been determined that welded joints are safe against dynamic stresses since the fracture energy values are higher than the 27 J (at -20 ^{0}C) value stipulated by the standard for position welds and weld metal.

ACKNOWLEDGMENTS

This study was supported by Gazi University Technology Transfer Office (TTO) and Birikim Engineering Design Center as project code 081251 STB. We thank both institutions.

CONFLICTS OF INTEREST

No conflict of interest was declared by the authors.

REFERENCES

[1] Maruf, H., Sam, P., Marko, H., Malcolm, P., “Calculating breakage parameters of a batch vertical stirred mill”, Minerals Engineering, 111: 229-237, (2017), DOI: https://doi.org/10.1016/j.mineng.2017.06.024

[2] Jankovic, A., “Fine grinding in the Australian Minerals Industry”, Journal of Mining and Metallurgy, 51-61, (2000).

[3] Hoyer, D., “Fine grinding with the tower mill: A comparison with a ball mill”, Mintek No, C336M, (1984).

[4] Rosa, A., Oliveira, P., Donda, J. D., “Comparing ball and vertical mills performance-an industrial case study, In: IMPC Proceedings”, Comminution Processes, 8: 44-51, (2014).

[5] Jankovic, A., "Variables affecting the fine grinding of minerals using stirred mills", Minerals Engineering, 16: 337-345, (2003).

[6] Danielle, R., Erik, S., Patrick, T., Hugh, M., "Predicting the product particle size distribution from a laboratory vertical stirred mill", Minerals Engineering, 129: 85-92, (2018). DOI: https://doi.org/10.1016/j.mineng.2018.09.016

[7] Stief, D., Lawruk, W., Wilson, L., "Tower mill and its application to fine grinding", Mining Metallurgy&Exploration, 4: 45-50, (1987). DOI: https://doi.org/10.1007/BF03402674

[8] Roitto, I., Lehto, H., Paz, A., Astholm, M., "Stirred milling technology-A new concept in fine grinding", Perth WA, (2013).

[9] Hasan, M. M., "Process modelling of gravity induced stirred mills. Ph. D. Thesis", University of Queensland, Brisbane, Australia, (2016).

[10] Priscila, M. E., Douglas, B. M., Roberto Galéryand Luís, C. R. M., "Industrial vertical stirred mills screw liner wear profile compared to discrete element method simulations, Minerals, (2021). DOI: https://doi.org/10.3390/min11040397

[11] Shi, F., Morrison, R., Cervellin, A., Burns, F., Musa, F., "Comparison of energy efficiency between ball mills and stirred mills in coarse grinding", Minerals Engineering, 22: 673-680, (2009). DOI: https://doi.org/10.1016/j.mineng.2008.12.002

[12] Cleary, P.W., Sinnott, M., Morrison, R., "Analysis of stirred mill performance using DEM simulation: Part 2-Coherent flow structures, liner stress and wear, mixing and transport", Minerals Engineering, 19: 1551-1572, (2006). DOI: https://doi.org/10.1016/j.mineng.2006.08.013

[13] Oliveira, A.L.R., Rodriguez, V.A., Carvalho, R.M., Powell, M.S., Tavares, L.M., "Mechanistic modeling and simulation of a batch vertical stirred millAuthor links open overlay panel", Minerals Engineering, 156:1-12 106487, (2020). DOI: https://doi.org/10.1016/j.mineng.2020.106487

[14] İnternet: Eirich, Brochure: EIRICH Tower Mill-Vertical Agitated Media Mill, Available online: https://www.eirich.com/fileadmin/user_upload/Eirich_Bilder/1.Produkte_Verfahren/2.Mahltechnik/5.TowerMill/TM1843_3_en.pdf (Accessed on 26 March 2024), (2018).

[15] Alım, YD., "Conveyor selection and design", Ankara: SEGEM, (1986).

[16] İnternet: Metso, Blog: When to change vertimill™ liners and how to do it safely!, Available online: https://www.metso.com/blog/mining/blog-when-to-change-vertimill-liners-and-how-to-do-it-safely/ (Accessed on 26.03.2024).

[17] Daraio, D., Villoria, J., Ingram, A., Stitt, E.H., Marigo, M., "Investigating grinding media dynamics inside a vertical stirred mill using the discrete element method: Effect of impeller arm length", Powder Technology, 364: 1049-1061, (2020). DOI: https://doi.org/10.1016/j.powtec.2019.09.038

[18] Jain, A.B., "Development of mathematical models to analyze and predict the weld bead geometry in submerged arc welding of low carbon alloy steel", International Journal on Emerging Trends in Mechanical & Production Enginee, 2(1): 2581-4486, (2018).

[19] Choudhary, A., Kumar, M., & Unune, D. R. (2019). Experimental investigation and optimization of weld bead characteristics during submerged arc welding of AISI 1023 steel. Defence Technology, 15(1), 72–82, (2019). https://doi.org/10.1016/j.dt.2018.08.004

[20] Vedrtnam, V.S., Singh G., Kumar, A., "Optimizing submerged arc welding using response surface methodology, regression analysis, and genetic algorithm", Defence Technology, 14(3): 204-212, (2018). DOI: https://doi.org/10.1016/j.dt.2018.01.008

[21] Abohusina, A., "Determining the optimum welding parameters on the weldability of mild steel using submerged arc welding process", (MSc). Department of Mechanical Engineering and Energies, School of Engineering and Applied Sciences, Libyan Academy for Post Graduate Studies, Janzur, Libya, (2018).

[22] Reddy, K.S., "Optimization & prediction of welding parameters and bead geometry in submerged arc welding", International Journal of Applied Engineering Research and Development (IJAERD), 3(3): 1-6, (2013).

[23] Avcı, T., "Spiral kaynaklı boru üretiminde kaynak otomasyonu", Yüksek Lisans Tezi, Yıdız Teknik Üniversitesi Fen Bilimleri Enstitüsü, İstanbul, (2008).

[24] Romina, C., David, R.I., Francesco, G., "Correction to: Submerged arc welding process: a numerical investigation of temperatures, displacements, and residual stresses in ASTM A516-Gr70 corner joined samples", The International Journal of Advanced Manufacturing Technology, 129: 3769, (2023). DOI: https://doi.org/10.1007/s00170-023-12617-1

[25] Anık, S., "Welding technology II submerged arc welding technique", Gedik Kaynak Sanayi Ticaret Anonim Şirketi, İstanbul, (1998).

[26] Külahlı, E., "Welding Science", Oerlikon Yayını, İstanbul, (1988).

[27] Kim, Y., Hwang, K.K., Kim, J.H., "Fracture behavior of heat-affected zone in low alloy steels", Journal of Nuclear Materials, 299(2): 132-139, (2001). DOI: https://doi.org/10.1016/S0022-3115(01)00688-2

[28] Sharma, P., Mohal, S., "Parametric Optimization of Submerged Arc Welding Process Parameters by Response Surface Methodology", Materialstoday Proceedings, 24(2): 673-682, (2020). DOI: https://doi.org/10.1016/j.matpr.2020.04.321

[29] Esteves, P.M., Douglas, B.M., Galéry, R., Machado, L.C.R., "Industrial Vertical Stirred Mills Screw Liner Wear Profile Compared to Discrete Element Method Simulations", Minerals**,** 11(4): 397, (2021). DOI: https://doi.org/10.3390/min11040397

[30] Kumar, A., Sahu, R., Tripathy, S.K., "Energy-efficient advanced ultrafine grinding of particles using stirred mills", A Review Energies, 16: 5277, (2023). DOI: https://doi.org/10.3390/en16145277

[31] Akay, A.A., "Joining of materials with different properties by submerged arc welding method and destructive and non-destructive examination of the joints", Karabük Üniversitesi Fen Bilimleri Enstitüsü Yüksek Lisans Tezi, Karabük, (2012).

[32] Zhang, M., Han Y., Jia C., et al "Improving the microstructures and mechanical properties with nano-Al2O3 treated wire in underwater submerged arc welding", Journal of Manufacturing Processes, 74: 40-51, (2022). DOI: https://doi.org/10.1016/j.jmapro.2021.11.056

[33] Edwin Raja Dhas, J., Anton Savio Lewise, K., Laxmi, G., "Submerged arc welding process parameter prediction using predictive modeling techniques", Matertoday Proceedings, 64: 402-409, (2022). DOI: https://doi.org/10.1016/j.matpr.2022.04.757

[34] Benedetti, M., Fontanari, V., Santus, C., "Crack growth resistance of MAG butt-welded joints of S355JR construction steel", Engineering Fracture Mechanics, 108: 305-315, (2013).

[35] İnternet: CEMA, "Screw conveyors for bulk materials", https://cemanet.org/wp-content/uploads/2019/06/EC-2019-Bulk-Handling-Section-Meeting-Agenda-set.pdf (Accessed on 26 March 2024).

[36] Forcade, M., "Screw conveyor 10", Goodman Conveyor Company, (1999).

[37] Alışverişçi, M., "Belt conveyors", İstanbul, (1985).

[38] Nogay, M.N., "Screw conveyors design criteria", Yıldız Teknik Üniversitesi Fen Bilimleri Enstitüsü Makine Müh. Böl. Yüksek Lisans Tezi, İstanbul, (2007).

[39] Seshagiri, S., Krishna Moorthi, M., "Electrode extruder using screw conveyor", https://journals.pen2print.org/index.php/ijr/article/view/2126

[40] Mcgrath, JT., Chandel, RS., Orr, RF., Gianetto, JA., "Microstructure/Mechanical Property Relationships in Thick-Section C-Mn Narrow-Groove Welds", Weld Journal, 67: 196-201, (1988).

[41] Miyamoto, G., Karube, Y., Furuhara, T., "Formation of grain boundary ferrite in eutectoid and hypereutectoid pearlitic steels", Acta Materialia, 103: 370-381, ISSN 1359-6454, (2016), https://doi.org/10.1016/j.actamat.2015.10.032

[42] Song, HY., Evans, GM., Babu, SS., "Effect of microstructural heterogeneities on scatter of toughness in multi-pass weld metal of C-Mn steels", Science and Technology of Welding and Joining, 19(5): 376-384, (2014). DOI: https://doi.org/10.1179/1362171814Y.0000000194

[43] Gürol, U., Çoban, O., Coşar, İ.C., Koçak, M., "Effect of the notch location on the Charpy-V toughness results for robotic flux-cored arc welded multipass joints", Materials Testing, 64(9): 1278-1289, (2022). DOI: https://doi.org/10.1515/mt-2022-0113

[44] Maksuti, R., "Impact of the acicular ferrite on the Charpy V-notch toughness of submerged arc weld metal deposits", International Journal of Scientific & Engineering Research, 7(8): 1149-1155, (2016).

[45] Akkaş, N., Onar, V., Varol, F., "Microstructure Analysis of Resistance Spot Welding of S235JR(Cu) Steel Sheets Used in Rail System Vehicles", 3rd International Congress of Vocational and Technical Sciences, Gaziantep, 1591-1599, (2018).

[46] Çetinkaya, C., Akay, A., Arabacı, U., Fındık, T., "Effect of primer coating applied to S235JR material on submerged arc weldability", Journal of Polytechnic, 25(3): 1335-1348, (2022). DOI: http://doi.org/10.2339/politeknik.1119093

[47] Varola, A., Bozana, MS., Çoband, O., Gürola, U., "The influence of filler wire on microstructure and mechanical properties is submerged arc welding of S355J2 structural steel", Journal of Innovative Engineering and Natural Science, 4(2): 426-438, (2024). DOI: http://doi.org/10.61112/jiens.1415708

[48] Gook, S., Midik, A., Biegler, M., Gumenyuk, A., Rethmeier, M., "Joining 30 mm Thick Shipbuilding Steel Plates EH36 Using a Process Combination of Hybrid Laser Arc Welding and Submerged Arc Welding", Journal of Manufacturing and Materials Processing, 6(4): 84, (2022). DOI: https://doi.org/10.3390/jmmp6040084

[49] Üstündag, Ö., Avilov, V., Gumenyuk, A., Rethmeier, M., "Full penetration hybrid laser arc welding of up to 28 mm thick S355 plates using electromagnetic weld pool support", Beam Technologies and

Laser Application IOP Publishing IOP Conf. Series: Journal of Physics: Conference Series 1109 012015, (2018). DOI: https://doi.org/10.1088/1742-6596/1109/1/012015

[50] Paz, A., Zhmarin, E., Polske, H., "Recent Developments In Coarse Grinding Using Vertical Stirred Mills", Swiss Tower Mills Minerals AG, Comminution 23 Draft Papers, Switzerland, (2023).

[51] Paz, A., Ypelaan, C., T., Ryan, M., McIness., "The Application of Ultra Fine Grinding for Sunrise Dam Gold Mine, Paper presented in Millops", Mill Operators Conference, Brisbane, Queensland, Australia, (2021).

[52] Paz, A., Ghattas, G., Loro, S., Belke, B., "Fine Grinding Implementation at the Cracow Gold Processing Plant", Paper presented in Metplant 2019, Perth, Western Australia, (2019).

[53] Sailender, M., Suresh, R., Reddy, GC., Venkatesh, S., "Prediction and comparison of the dilution and heat affected zone in submerged arc welding (SAW) of low carbon alloy steel joints", Measurement, 150: 107084, ISSN 0263-2241, (2020). DOI: https://doi.org/10.1016/j.measurement.2019.107084

[54] Mazzinghy, D., Schneider, C., Alves, V., Galery, R., "Vertical agitated media mill scale-up and simulation", Minerals Engineering, 73, 69-76, (2015).

[55] Mcgrath, JT., Chandel, RS., Orr, RF., Gianetto, JA., "Microstructure/Mechanical Property Relationships in Thick-Section C-Mn Narrow-Groove Welds", Weld Journal, 67: 196-201, (1988).

[56] Miyamoto, G., Karube, Y., Furuhara, T., "Formation of grain boundary ferrite in eutectoid and hypereutectoid pearlitic steels", Acta Materialia, 103: 370-381, ISSN 1359-6454, (2016). DOI: https://doi.org/10.1016/j.actamat.2015.10.032.

[57] Edwin Raja Dhas, J., Anton Savio Lewise, K., Laxmi, G., "Submerged arc welding process parameter prediction using predictive modeling techniques", Materialstoday: Proceedings, 64(1): 402-409, (2022). DOI: https://doi.org/10.1016/j.matpr.2022.04.757

[58] Kaluç, E., "Melting based welding methods", Makine Mühendisleri Odası Kocaeli Şubesi, Kaynak Teknolojisi El Kitabı Cilt 1 Yayın No:356, Kocaeli, (2004).

[59] Sarfudeen, M., Muthukumaran, S., "Effect of cold wire addition on improvement in productivity by submerged arc welding in wind turbine tower fabrication", Materialstoday: Proceedings, 27(3): 2699-2702, (2020). DOI: https://doi.org/10.1016/j.matpr.2019.12.185

[60] Byeong, C.G., "Effect of Post-Weld Heat Treatment on the Fatigue Behavior of Medium-Strength Carbon Steel Weldments", Metals, 11(11): 1700, (2021). DOI: https://doi.org/10.3390/met11111700

[61] Wieczorska, A., Domżalski, R., "The influence of submerged arc welding conditions on the properties of S355JR structural steel joints", International Journal of Mechanical Engineering and Technology (IJMET), 12(12):19-29, (2021). DOI: https://doi.org/10.17605/OSF.IO/E32PV

[62] Wieczorska, A., Labuda, W., "Analysis of the process of qualifying the welding technology of S355JR structural steel using the submerged arc welding method", Journal of Achievements in Materials and Manufacturing Engineering, 118(1): 18-27, (2023). DOI: https://doi.org/10.5604/01.3001.0053.7287

[63] Wieczorska, A., Abramczyk N., "Developing technology for the welding of steam turbine steering diaphragms using the submerged arc welding method", Journal of KONBiN, 52(3): 233-245, (2022). DOI: https://doi.org/10.2478/jok-2022-0035

[64] Quan, C., Jiang, Y., Xinghui, L., Jingli, T., "Bensheng Huang Effect of the groove type when considering a thermometallurgical-mechanical model of the welding residual stress and deformation in an S355JR-316L dissimilar welded joint", Journal of Manufacturing Processes, 45: 290-303, (2019). DOI: https://doi.org/10.1016/j.jmapro.2019.07.011

[65] Balakrishnan, M., Leitão, C., Craveiro, D., Rodrigues, D.M., Santiago, Silva, A., L.S. and Subramanian, C., "Post fire tensile properties of S355 J2 structural steel welded connections for construction industrial applications", Metallurgical Research & Technology, 119:511, (2022). DOI: https://doi.org/10.1051/metal/2022056

[66] İrsel, G., "Study of the microstructure and mechanical property relationships of shielded metal arc and TIG welded S235JR steel joints", Materials Science and Engineering: A, 830:142320, (2022). DOI: https://doi.org/10.1016/j.msea.2021.142320

[67] Şık, A., Önder, M., "Comparison between mechanical properties and joint performance of AA 2024-O aluminium alloy welded by friction stir welding and TIG processes", Kovove Material, 50:131-137, (2012). DOI: https://doi.org/10.4149/km_2012_2_131